Computer Methods and Programs in Biomedicine (2004) **76**, 229—238

ELSEVIER

Computer Methods and Programs in Biomedicine

www.intl.elsevierhealth.com/journals/cmpb

A study on the reference electrode standardization technique for a realistic head model

Yiran Zhai, Dezhong Yao*

School of Life Science and Technology, University of Electronic Science and Technology of China, Chengdu 610054, PR China

Received 8 June 2004; accepted 30 July 2004

KEYWORDS
Reference electrode standardization technique;
Equivalent source technique;
Reference at infinity;
Average reference

Summary One oldest technical problem in EEG practice is the effect of an active reference on EEG recording, and it is especially important for identifying the temporal information of EEG recordings. To solve this problem, a reference electrode standardization technique (REST) has been proposed for a concentric three-sphere head model. REST, based on an equivalent distributed source model, reconstructs the potential with a reference at infinity from the potential with a scalp point reference or with the average reference. In this paper, investigated was the REST for a realistic head model. The results of simulation studies show that the potential reconstruction for the realistic head model is more sensitive to noise than that for the concentric three-sphere head model, so a regularized inverse by truncated singular value decomposition was introduced. The results confirm that REST is still an efficient method even for a realistic head model especially for the most important superficial cortex region.

1. Introduction

Both the evoked potential (EP) and the spontaneous potential (EEG) of neural activities are currently read in terms of components thought to reflect distinct neural generators [1,2]. One of the most important characteristics to define these components is potential. However, only the difference between two potentials can be measured, so it is indispensable to set a reference in human scalp recordings [3]. Therefore, the current cephalic electrode, non-cephalic electrode, earlobe reference, neck reference, average reference etc. each yields some effects on the recordings. As neural electrical activation is a spatio-temporal process, the effects of an active reference may be in both spatial and temporal aspects. To solve this problem, a neutral potential is desired to act as the reference. However, it is almost impossible to find a point of neutral or zero potential on a body

* Corresponding author. Tel.: +86 28 83206124; fax: +86 28 83206124.
E-mail address: dyao@uestc.edu.cn (D. Yao).

0169-2607/$ — see front matter © 2004 Elsevier Ireland Ltd. All rights reserved.
doi:10.1016/j.cmpb.2004.07.002

surface [1,4,5]. Physically, the potential at infinity is the ideal reference since a point at infinity is far from all the neural sources, thus bringing no effect on EEG recordings, and the work reported here is our on-going effort to establish such a reference.

2. Background

Recently, a software method, termed REST (reference electrode standardization technique), was proposed to approximately transform a scalp reference point or the average reference to a reference point at infinity [6]. The transformation is based on the bridge—the common origin of the two potentials before and after transformation, i.e. the actual neural sources or their equivalent sources [7,8]. It is a latent method from the results of the simulations of three-concentric-sphere model. In this paper, the technique was evaluated for a realistic head model and special consideration is made onto the effect of noise.

3. Computational method and theory

3.1. Realistic head model and the equivalent source technique

The scalp potentials can be represented as:

$$V = GX \tag{1}$$

where the matrix V with size $l \times k$ represents scalp potential recordings at l electrodes with k samples, the matrix X with size $m \times k$ represents k samples of m neural source signals in the head model, and the matrix G with size $l \times m$ is the transfer function determined by the head model, source model and electrode montage. The transfer matrix is derived with indirect boundary element method (BEM) [9,10].

If the inverse of the transfer matrix in Eq. (1) exists, the sources can be correctly reconstructed from the recordings. However, it is very difficult for an EEG inverse problem to determine simultaneously the number of sources and their locations, strengths and orientations, and there is a theoretical limitation that the solution to the EEG inverse problem is non-unique. In fact, it is the non-uniqueness that provides the theoretical base of the equivalent source technique (EST) [6], which is utilized to recover the scalp potentials with reference at infinity in this work. Here the equivalent dipole layer was chosen as the equivalent sources of the actual sources for its simplicity in realization and relatively better performance. In order to have a good approximation of the continuous dipole layer, the number of the equivalent sources is generally much larger than the scalp recording number l, so the problem is an underdetermined problem. The unique minimum norm linear inversion is the general choice for such a problem to obtain the discrete equivalent distributed sources [11] and such an inversion can be easily conducted by a general inverse of the transfer matrix, such as the singular value decomposition (SVD) algorithm [6]. In this work, a truncated SVD (TSVD) was used to decrease the effect of noise.

In our previous work, a three-concentric-sphere model was adopted as the head model [6]. In this study a three-layer realistic head model was used. The realistic head model was reconstructed from MRI images and triangularly shaped [10,12]. As

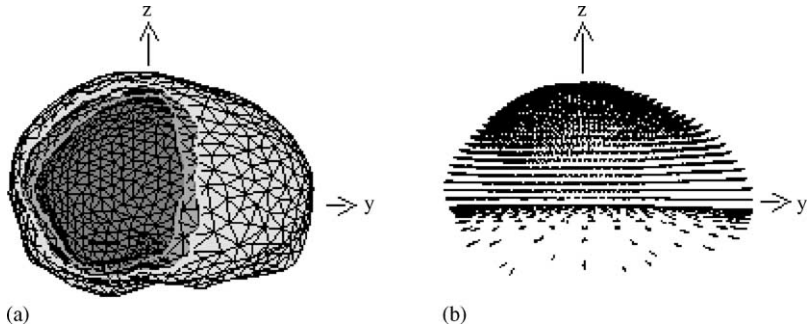

Fig. 1. Realistic head volume conductor model and the 3000 radical dipoles. It is a sagittal plane along x-axis of the three-layer realistic head model. The axis directing from the right ear to the left ear is defined as $+x$ axis and that from the nasion to the afterbrain is $+y$ axis. The $+z$ axis is defined as the axis from neck to vertex with the unit centimeter. (a) The three-layer realistic head model. The blackest part represents the brain layer and the shallow part represents the scalp layer. The conductivities are 1.0 (brain and scalp) and 0.0667 (skull). (b) The 3000 radical dipoles on the assumptive equivalent source layer.

shown in (a) of Fig. 1, the outer layer is the scalp, the intermediate one is the skull and the inner one is the brain, while the conductivities are 1.0 (brain and scalp) and 0.0667 = 1/15 (skull) [13]. There are 700, 799 and 1027 nodes and 1396, 1594 and 2050 triangles in the three layers of the realistic model, respectively. An assumed equivalent dipole layer was constructed by contracting the brain layer to 90% of its size and there are 3000 radial dipoles distributing on the surface. Each dipole is represented by '↑' and the 3000 radial dipoles are shown in Fig. 1(b).

3.2. REST algorithm and procedure

Based on EST [6,14], the sources X in Eq. (1) may be either the actual sources or their equivalent dipole sources; here they are assumed to be the equivalent dipole sources, then using Eq. (1) and

$$V_a = V - \boldsymbol{t}\boldsymbol{v}_a = G_a X \tag{2}$$

we obtain

$$V = GX \approx V' = G(G_a^+ V_a) = R_a V_a \tag{3}$$

Here V_a is scalp EEG recording with average reference, $\boldsymbol{t}$ is a column vector with size $l \times 1$ and each of its elements being unity, $\boldsymbol{t}'$ is the transpose of $\boldsymbol{t}$, $\boldsymbol{v}_a$ is the average of the scalp potentials and $\boldsymbol{v}_a = \frac{1}{l}\boldsymbol{t}'V$, V' is the approximately restored V by using the approximately reconstructed equivalent sources $X \approx G_a^+ V_a$, sign '+' denotes the general inverse which is obtained by SVD in the following simulation study [6], the matrix R_a is the average reference standardization matrix. For the earlobe reference recordings, we have

$$V_e = V - \boldsymbol{t}\boldsymbol{v}_e = G_e X \tag{4}$$

correspondingly

$$V = GX \approx V' = G(G_e^+ V_e) = R_e V_e \tag{5}$$

where $\boldsymbol{v}_e$ is the potential at the earlobe referenced at infinity and is a row vector in V corresponding to the reference electrode, R_e is the earlobe reference standardization matrix. R_a and R_e are determined by four factors: the volume conductor model, the equivalent source model, the electrode montage and the calculation of the general inverse.

As $V = V_a + \boldsymbol{t}\boldsymbol{v}_{a'}$, $V' = V'_a + \boldsymbol{t}\boldsymbol{v}'_a$ and we know V_a, the result of the standardization is further chosen to be

$$V' = V_a + \boldsymbol{t}\boldsymbol{v}'_a \tag{6}$$

Apparently, the error between V_a and the standardized V'_a is avoided by using Eq. (6) as the final result, and the remaining error is only the difference between the objective $\boldsymbol{v}_a$ and the restored $\boldsymbol{v}'_a$.

The procedures are as follows:

- The electrode montage is given and the scalp recordings V_a is got by experiments or calculated in simulations. A realistic head model such as the model shown in Fig. 1 (a) are reconstructed from individual MRI images and an equivalent source model such as the discrete dipole layer source model shown in Fig. 1(b) are assumed.
- Based on the above electrode montage, realistic head model and equivalent source model, calculate the transform matrix G in Eq. (1) and G_a in Eq. (2) by BEM.
- Calculate the general inverse G_a^+ of the matrix G_a by TSVD, and calculate the standardization matrix R_a in Eq. (3) from G_a and G_a^+.
- Calculate the $V' = R_a V_a$ as shown by equation (3), and then calculate $\boldsymbol{v}'_a = \text{average}(V')$.
- Calculate the final reconstructed EEG recording V' according to Eq. (6) by the known recording V_a and the recovered $\boldsymbol{v}'_a$.

For earlobe reference, the calculation process is similar.

The program was developed under Matlab 6.1 and it may be run on Windows 9x/NT/2000 systems.

3.3. Simulation procedure

In theory, it is difficult to reconstruct the strict equivalent closed dipole layer from the EEG recordings with limited number of electrodes on the scalp. Therefore, a practical discrete dipole layer is approximately equivalent to the inner neural source in the brain and the equivalence depends on the direction and the position of inner dipole sources. Therefore, the effectiveness of REST depends on the direction and position of inner dipole sources and it is important to investigate the effectiveness by simulations.

The temporal process of a dipolar neural source was simulated by a damped Gaussian function

$$h(t_i) = \exp\left(-\left(2\pi f \frac{t_i - t_0}{\gamma}\right)^2\right) \cos(2\pi f(t_i - t_0) + \alpha), \quad i = 1, \ldots, k \tag{7}$$

where $t_i = i \times \mathrm{d}t$, $k = 256$ and $\mathrm{d}t = 0.004\,\mathrm{s} = 4\,\mathrm{ms}$. We chose this function just because it looks like an evoked potential. The values of parameters t_0, f, γ and α are shown in the following sections for each concrete case. Here t_0 denotes the delay of the peak, f denotes the main frequency, γ controls the decay of the waveform, and α denotes a phase

constant. Using the function h and the above forward model Eqs. (1), (2) and (4), we derived the spatio-temporal recordings V, V_e and V_a. The relative error (RE) is used to evaluate the effectiveness of REST, and it is

$$\mathrm{RE} = \frac{\|V - V_*\|}{\|V\|} \tag{8}$$

where V is the forward spatio-temporal recording with reference at infinity, and V_* is an alternative of the recording V_a, V_e and V'. The matrix norm $\|*\|$ is defined as $\|V\| = (\sum_i \sum_{j=1}^{k} v_{ij}^2)^{1/2}$. V and V_* generally correspond to the total l channels and sometimes are also used as single-channel signals to obtain the channel-based RE in the following calculations.

Since, the transformations shown by Eqs. (3), (5) and (6) from V_a or V_e to V are linear operations; we only need to check the performance according to the potential of a single dipole and noise independently. To understand the effectiveness of REST for different dipole locations and orientations, simulations were conducted for each voxel of a discrete cubic grid as a source position with each of the three unit dipoles (*Px*, *Py*, *Pz*) directed along the three Cartesian coordinate (*x*, *y*, *z*) directions separately. The inner cortex space is composed of 674 voxels and the grid started at (*x*, *y*, *z*) = (0.0, 0.0, 0.0) with inter-grid distance of 1 cm. The total dipoles tested are 674 (voxels) $\times$ 3 (dipoles at each voxel) = 2022, and for each of the 2022 dipoles we obtained the V, V_a and V_e. Then we obtained the V' by Eqs. (3) (or (5)) and (6), and an RE (average), an RE (earlobe) and an RE (standardization) pertaining to $V_* = V_a$, $V_* = V_e$ and $V_* = V'$ in Eq. (8), respectively. In short, for each voxel, we obtained nine REs pertaining to the three dipoles (*Px*, *Py*, *Pz*) and three references (average, earlobe and standardization).

4. Simulation study (I): effectiveness of rest

4.1. Comparison between earlobe reference and average reference

In this simulation, a left earlobe reference was assumed at scalp location (*x*, *y*, *z*) = (0.8529, 8.356, 1.4053) and the parameters in Eq. (7) were t_0 = 35 $\times$ dt, f = 10Hz, γ = 5 and $\alpha = \pi/2$. The upper row in Fig. 2 is a slice display of the volume distribution of RE (earlobe), and the lower row of Fig. 2 is a slice display of the volume distribution of RE (average). Apparently, RE (earlobe) depends not only on the dipole orientation (the differences among the three figure parts in the upper row) and dipole location (the non-constant value in each figure part), but also on the reference site (the RE distribution in each of the three figure parts is clearly around the reference position). The reason is that the smaller the distance between the source and the left earlobe, the larger value of the distortion caused by subtracting v_e is. Comparing RE (earlobe) with RE (average), we find that the largest RE of RE (earlobe) (337% of a *Py* dipole) is much larger than that of RE (average) (91.4% of a *Pz* dipole). In

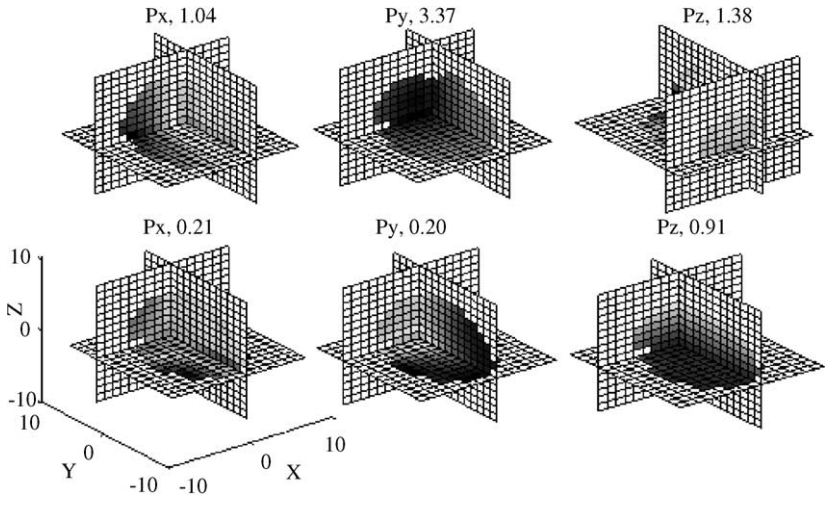

Fig. 2. Slice display of the volume distribution of RE. The upper row shows RE (earlobe) between the potential with a reference at infinity and that with the left earlobe reference. The lower row shows RE (average) between the potential with a reference at infinity and that with the average reference. *Px*, *Py* and *Pz* indicate the dipole sources orientated along the three Cartesian coordinates: *x*-axis, *y*-axis and *z*-axis, respectively. The white point is zero and the blackest point is the maximum value as show over each figure part. The unit is centimeter.

addition, we found the largest RE (average) 20.9% of *Px* dipoles is almost the same as the largest RE (average) 19.9% of *Py* dipoles, while the largest RE (earlobe) 104% of *Px* dipoles is distinctly different from the largest RE (earlobe) 367% of *Py* dipoles, and these differences between the average and the earlobe or a scalp point reference provide the basic reasons for that the average reference is more widely used in current EEG/ERP practice.

4.2. Effect of noise and regularization

Due to the linearity of Eqs. (3) and (5), and in order to understand the noise effect independently, simulations using only noise as the input to the standardization operator R_a were carried out in this work. A Gaussian white noise is used to simulate the noise of the environmental and the mechanical noise. According to Eqs. (3) and (6), we obtain $N' = N + \boldsymbol{t}$ average (N'). Where 'average' means the average of the recordings over all sensors sample by sample temporally, and here we assume average (N) = 0. From the noise simulations for realistic head model, we found that 'average (N')' changes with different singular-value truncations. This means that when noise exists in the data, the standardization may introduce an instantaneous constant value to each channel. Hence, a proper regularization is necessary to reduce the effect of noise.

The condition number (CN) is defined as the ratio of singular value pertaining to the truncation point to the first value that is the largest. Fig. 3 shows the distribution of CN of G_a in Eq. (3) and the result of REST with different truncations. Fig. 3(a) shows 128 CN of the transfer matrix G_a for the 128-electrode montage and 3000 equivalent dipoles. We found that CN change smoothly from CN (1) = 1.00 to CN (128) = 0.00. Fig. 3(b) shows the change of REs while setting different truncations. The curve of '*' represents the changes of RE for different CNs and RE is calculated by Eq. (8) with $V = N$ and $V_* = N'$. Hence, RE can represent the effect of noise for a realistic model and CNs are selected ranging from 0.00001 to 1. From Fig. 3(b), we can find the minimum RE = 0.44 while CN (53) is 0.0135. In this paper, 0.0135 was adopted as CN to calculate G_a with 128 electrodes used for a realistic head model.

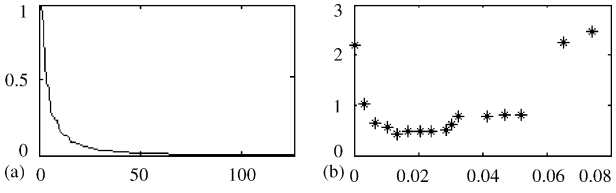

Fig. 3. The CN curve of G_a and the results of different truncations. (a) The curve shows the 128 normalized CNs of G_a. (b) REs of different truncations. The '*' curve shows REs change according to different CNs with the abscissa being CNs and ordinate being value of REs.

We calculated the R_a with CN equals 0.0135 (truncated at the 53th singular values) and implemented a noise test example. The standard deviation and mean value of the original input noise is 1.00 and 0.01, while the counterparts of the output N' are 1.22 and 0.04. The ratio between 1.22 and 1.00 is 1.2 and the difference between the averages is 0.03. These facts mean that the total noise content is kept approximately the same in the transformation. However, the difference between N and N', the average (N'), is different from one moment to another. The total RE is 46.1% calculated by Eq. (8) with $V = N$ and $V_* = N'$, and if RE is calculated channel by channel, then the maximum channel-based RE is 50.3% at channel 104 and the minimum is 41.2% at channel 29 in this example. In Fig. 4, N (original noise) and N' (transformed noise) are illustrated on the left and in the middle by their values in 128 channels at an instant, the difference, i.e. average (N') at this instant, between them are 0.19 at each channel position. However, the value average (N') is different from one instant to another as shown on the right of Fig. 4 (256 latency points), which looks like a random series with standard deviation and mean value being 0.24 and 0.04, respectively.

If the average (N) were zero, the standardization should not introduce a non-zero average (N'). However, REST is based on the prior assumption that the sources of the recordings are inside the equivalent dipole layer, and the net noise recordings are not able to be considered as potentials generated by sources inside the closed equivalent layer, so they cannot be standardized to a point at infinity by REST. For the using of V_a in Eq. (3), the net noise recordings are assumed to be the potentials

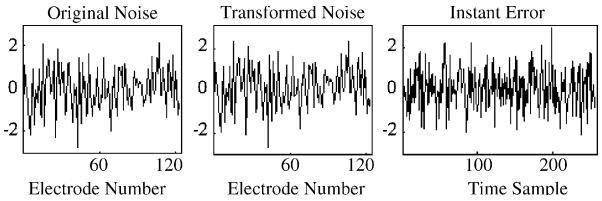

Fig. 4. The effect of noise. On the left (original noise) is an instantaneous noise distribution of the 128 electrodes, in the middle (transformed noise) is the output of the original noise undergoing the standardization operation, and their difference is 0.19 at each electrode position. On the right is the curve of the difference time course of the 256 instant noises introduced by REST in our study, where the first point is 0.19.

produced by sources inside the closed equivalent layer. Accordingly the standardization recovers an 'average (N')'. The value of 'average (N')' can be controlled by proper truncations.

4.3. RE distribution

Due to that the information contained in the potentials with average reference is the same as that with earlobe reference [6], the standardization result from an earlobe reference was almost the same as that from the average reference, and so, from now on, only the results for the average reference are shown. All REs of voxels created in the brain region were calculated. Only three middle slices of REs of the whole brain region are shown and they are the xoy, yoz and xoz planes projected onto three surfaces of the cube.

Fig. 5 shows the RE distribution along *x*-axis, *y*-axis and *z*-axis in the inner brain space. The upper row shows RE (average), and the lower one illustrates RE (standardization). RE (average) is caused by the deviation of the average of scalp potentials from zero assumed in the average reference recording model, and this deviation is different for a dipole at different locations with different orientations. The larger the deviation is, the larger RE is. We can find that RE (average) of a *Pz* dipole is always much larger than that of a *Px* or a *Py* dipole. The largest RE (average) of *Pz* dipoles is about 91.5%, and the smallest RE (average) of *Pz* dipoles is about 54.9%. However, the largest REs (average) of *Px* and *Py* dipoles are about 25.70% and about 22.6%, respectively, and their smallest values are almost zero. The reason is that a cap electrode montage mainly covers either the potential of the positive pole or that of the negative pole of a vertical dipole (*Pz*), so the average of the potential is usually distinctly different from zero. However, a cap electrode montage generally covers the potentials of both the positive and negative poles of a transverse dipole (*Px*, *Py*), so the average of the potentials is usually closer to zero than that of a vertical dipole (*Pz*).

The lower row of Figs. 5 and 6 is the result of REST from potentials with the average reference. The effectiveness of REST is revealed by the difference between the upper row and lower row of each figure. Based on these figures, we have the following. (1) If the original RE (average) is large such as RE (average) of a *Pz* dipole, REST is very effective as shown by the third column of Fig. 5. (2) The dependence on the source location is different between RE (average) and RE (standardization). For RE (average), the large REs (average) of *Px* and *Py* dipoles are in the shallow brain region, while for RE (standardization), the large REs (standardization) of *Px* and *Py* dipoles are in the deep brain region. This means REST is specifically efficient for the most important superficial cortex region.

To study the effects of electrode number, the similar simulations with both 64 and 32 electrodes had been done. Comparing the omitted results

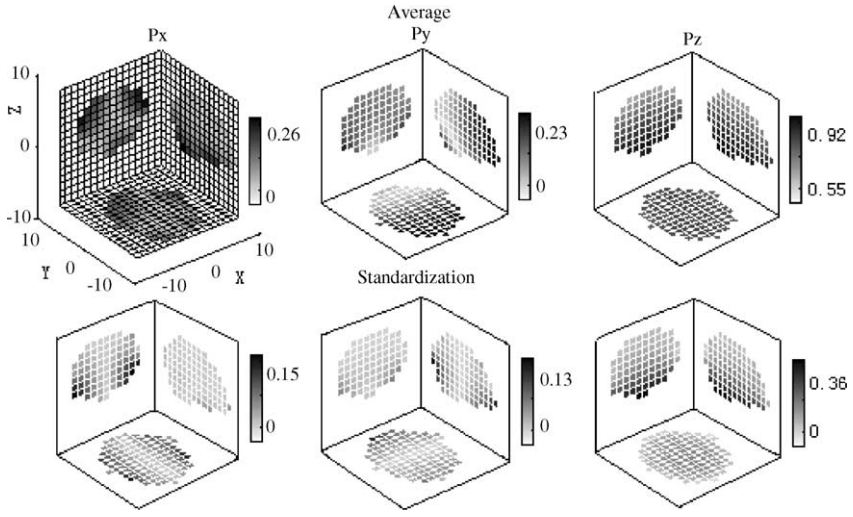

Fig. 5. The distribution of RE. Each map is a section distribution of REs. RE (average) is shown by the upper row of each figure part and RE (standardization) is shown by the lower row. Each section is one of the middle xoy, yoz and xoz planes projected onto three surfaces of the cube. The grids of each map are hidden for a clear display except for the left one of the upper row, which is shown with axes and grids. The white point corresponds to the smallest value; the blackest point corresponds to the maximum value. The three columns correspond to dipoles with orientations along *x(Px)*, *y(Py)* and *z(Pz)* axes respectively. The 128 electrodes are uniformly distributed on the scalp.

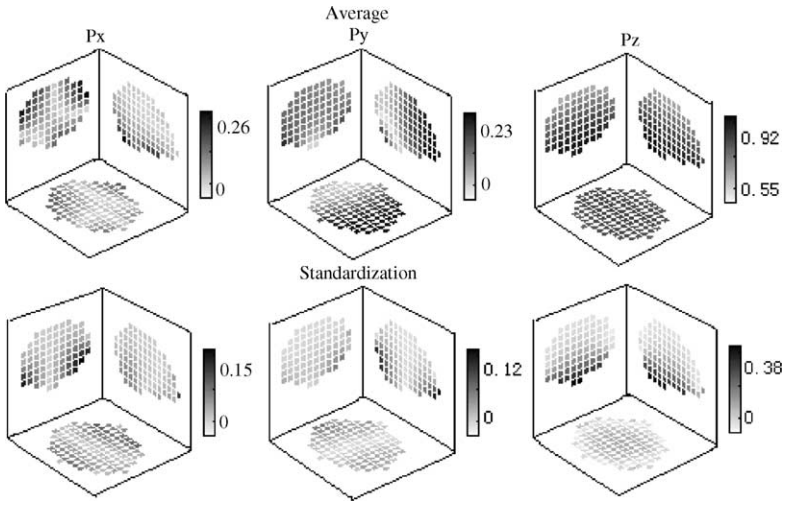

Fig. 6. Effects of conductor head model. It is the situation where the conductivities of the three layers in the realistic head model are 1.0 (brain, skull and scalp). The meanings of other parameters are the same as those in Fig. 5.

figures with Fig. 5, no much differences is found except that a denser electrode array is better for REST to reduce REs(average) as reported in the study of a three-concentric-sphere model [6]. In general, a dense electrode array is better than a sparse array in reducing RE (average) of a *Pz* dipole, while the efficiency difference between a dense and a sparse array is not very distinct in reducing REs (average) of *Px* and *Py* dipoles.

4.4. Effects of volume conductor model

The effects of the volume conductor model were evaluated by two assumptions. One is that the V_a is calculated by using the above-noted realistic head model, and the other is that the reference standardization matrix R_a in Eq. (3) is formed from a different model. In this test, we have assessed a case of a modified realistic model with the same conductivity 1.0, i.e. it is the situation where the conductivity of the skull layer in the realistic head model is modified to 1.0. 128 electrodes were used in the calculation and Fig. 6 shows the results. The basic characteristics are the same as those shown in Fig. 5, i.e. RE (average) in shallow region is larger than RE (standardization), but the difference and the effectiveness of REST are not so distinct as that shown by Fig. 5. For example, REs (standardization) of *Pz* dipoles in the deep cortex region using the modified head model (Fig. 6) are a little larger than those using the correct realistic head model (Fig. 5). These results on one hand mean that a detailed head model is preferred to an approximate head model for good reference standardization, and on the other hand they show that the standardization is still beneficial even using a modified head model in reducing RE.

5. Results of simulation study (II): significance of REST in temporal analysis

5.1. Dynamic effect of the average artefact

The temporal and frequency analysis are related to the reference, because a scalp point reference or the average reference for EEG varies with each latency. This section shows the dynamic effect of the average artefact and the effectiveness of REST in removing the average artefact. For the time courses and the spectra, the differences of the simulated EEG recordings with a reference at infinity, the average reference and the recovered EEG recordings with a reference at infinity are calculated. Suppose there are three dipoles in the volume conductor. They locate at $(-2.1, -1.05, 2.63)$ (r = 3.522), $(-1.05, 2.1, 3.15)$ (r = 3.929) and $(-1.58, -0.53, 3.68)$ (r = 4.325), respectively, and all are radial dipoles. The strength of the first two is one unit, and that of the third one is half a unit. The temporal process is defined by Eq. (7) with the parameters $t_0 = 35 \times dt$, f = 10Hz, γ = 5, $\alpha = \pi/2$ for dipole 1, $t_0 = 40 \times dt$, f = 6Hz, γ = 4, $\alpha = \pi/2$ for dipole 2 and $t_0 = 50 \times dt$, f = 20Hz, γ = 6,α = 0 for dipole 3.

The recordings of 10 electrodes are shown in Fig. 7. Their serial numbers among the 128 electrodes are shown, which are selected from channel 1 with an interval of 16 except channels 90 and 3.

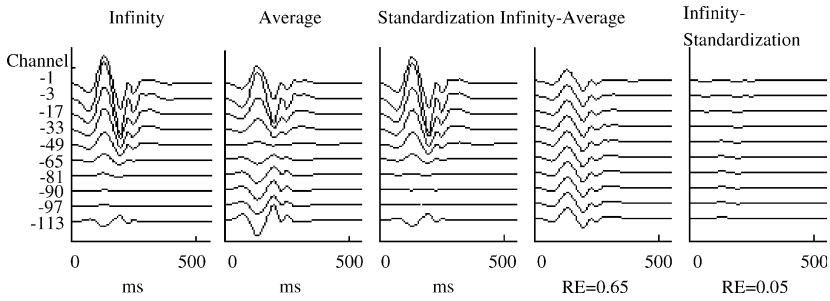

Fig. 7. Simulated scalp recordings and standardization result of time course analysis. The horizontal axis is in milliseconds. The channel order number is shown on the left of the first column. From left to right, the first is the recording with reference at infinity, followed by the average reference, and then the reference at infinity (standardization). The last two are the two differences infinity-average and infinity-standardization.

If we check each channel with Eq. (8), we obtain the channel-based RE distribution. The maximum channel-based RE (average) and RE (standardization) are at channel 90 and the minimum channel-based RE (average) and RE (standardization) are at channel 3. Fig. 7 shows that the waveforms of recordings with average reference are distinctly different from those with reference at infinity, and the waveforms of the standardized recordings are almost the same as those with reference at infinity. The total RE (average) of 128 channels is 64.6%, and after standardization, the global RE (standardization) reduces to 6.5%. The channel-based RE is reduced from 28.5% (minimum)—1644% (maximum) to 2.9% (minimum)—165% (maximum), respectively. Therefore, the advantage of REST is shown again.

Fig. 8 shows the normalized strength of the Fourier spectra of the ten channels, where the desired potential referenced at infinity is distinctly different from the practical potential referenced at average. And such a great difference between the spectra of average reference data and that of the desired data referenced at infinity may result in a misleading in the explanation of the temporal dynamic process such as EEG rhythm analysis. Fig. 8 also shows that the actual spectra are nicely reconstructed, and such a result means that the spectral analysis of EEG can be possibly made more objective and realistic by the application of REST.

5.2. An empirical example

Figs. 9 and 10 show the results of an empirical example about spatial selective attention in visual fields. When the subjects attend the left visual field and the stimuli just flash on the left visual field, potentials of 120 electrodes are recorded by a NeuroScan system. Due to an obvious artefact in channel 86, only the remaining 119 channels are used in the calculation. The recordings are from −200 to 1200 ms time locked to the stimulation. Here, as the number, 119, and positions of electrodes are different from the above simulations, the *Ra* was reconstructed according to the practical 119-electrode montage with a realistic head model and the equivalent dipoles layer model used in Fig. 5.

Ten of the 119 channels are shown in Fig. 9. Their order numbers among the 119 electrodes are

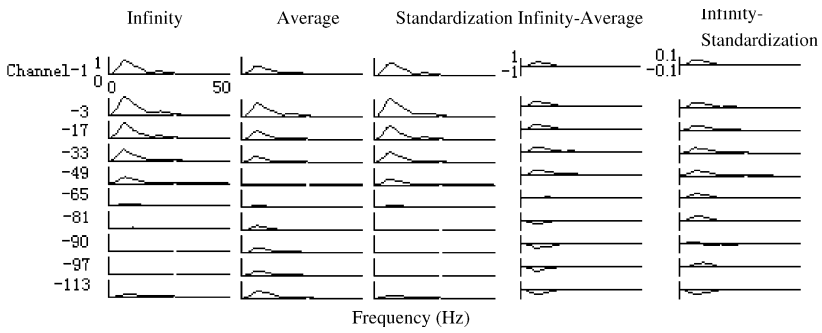

Fig. 8. Normalized strength of the Fourier spectra of the 10 scalp recordings shown in Fig. 7 The displaying range of the frequency axis is from 0 to 50 Hz. The values of the first three curves are normalized by the maximum value of each channel. The first three columns are displayed in the range [0—1] for they are always positive. The fourth column is displayed in the range [−1 to 1]. The fifth column is displayed in the range [−0.1 to 0.1] for its values are small.

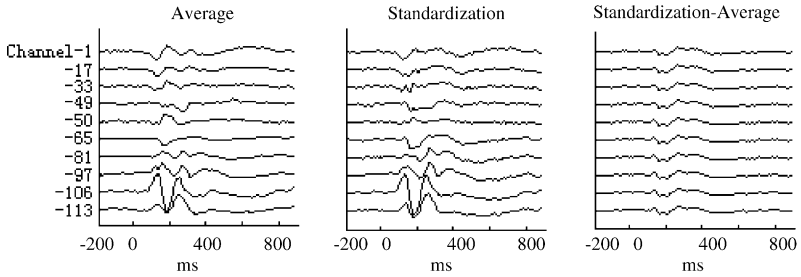

Fig. 9. Vivo VEP recordings. The abscissa is in milliseconds. The average is the practical recordings, the standardization is the result of the reference standardization. (The data were provided by the Beijing Key Laboratory of Cognitive Science, Chinese Academy of Sciences).

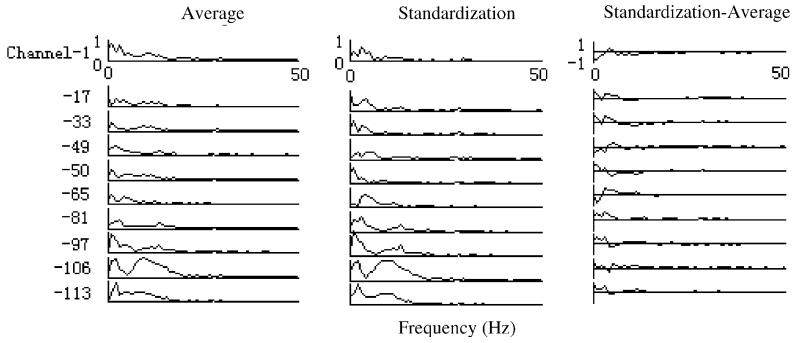

Fig. 10. Normalized spectrum display of the 10 scalp recordings shown in Fig. 9 The display range of the frequency axis is from 0 to 50 Hz. The value of each curve is normalized by the maximum value of each channel. The first two columns are displayed in the range of [0—1] for they are always positive. The third column is displayed in the range of[—1 to 1].

shown on the left, which are selected from channel 1 with an interval of 16 except channels 50 and 106. The average is the empirical recordings, the standardization is the result after standardization, and the standardization-average is the restored component. RE was calculated by Eq. (8) with V = standardization and V_* = average is 51.4%. The maximum channel-based RE is 119% occurring at channel 50 with Cartesian coordinates (x, y, z) = (—1.779, 7.619, 3.313) and the minimum channel-based RE is 23.49% occurring at channel 106 with Cartesian coordinates (x, y, z) = (—4.076, —4.937, 4.994). Viewing Fig. 9, the modification occurs not only in 'potential values' but also in polarity and latencies of peaks, and as such parameters are used in explanation of VEP data the standardization is of significance for VEP application.

Fig. 10 shows the spectra of the ten channels before and after standardization. We can find the variations of the spectra attributed to REST.

6. Conclusions and future plans

REST is a newly developed reference-free technique attempting to restore the lost potential of the reference electrode in EEG recordings. Since, equivalent sources can produce the same scalp potentials as the real sources inside the brain, and the equivalent sources can be approximately reconstructed by EST from the potentials with the average reference, the potentials with a reference at infinity can be approximately recovered. This is the fact on which REST is based. As the results of three-concentric-sphere model, simulations for a realistic head model also show that the reconstruction approximation of the equivalent sources is due to the imperfect information of the head model, limited scalp measurements and the regularization of matrix, and the degree of approximation is different for different source location and orientation. The most important result is that RE could be reduced for most brain source locations especially the most important upper superficial cortex region of the brain. That is to say, the reference effect could be reduced by REST and so an improvement of the temporal analysis including the spectral analysis could be made. Therefore, we are encouraged to believe this technique is likely to bring an impact on EEG research and clinical practice.

It is inevitable to face the ill-post transfer matrix for using indirect BEM to reconstruct the equivalent

source layer, which means a small quantity of noises in the measured potential may lead to the failure of the reconstruction. To resolve this problem, SVD is widely used. Using SVD for solving matrices, we are offered the option for selecting the number of singular values that are to be included in the signal space. The retained singular values should represent the signal or principal components since these are used for the equivalent source reconstruction. The discarded singular values should mainly represent the noise since this information is zeroed and does not factor into the reconstruction. What we have just done is a form of regularization known as truncated singular value decomposition (TSVD). If a reasonable truncation is specified, the regularization solution will be stable. In general, it is hard to find a criterion for proper truncation. From Fig. 3(b), it is found that the lower part of RE curve where we selected CN for truncation is flat and smooth. We have also conducted the simulations using CNs near 0.0135, whose values ranges from 0.0068 to 0.0304, i.e. from CN (71) to CN (35), and found no obvious difference. Therefore, CN can be selected in a comparatively large scope for calculation without much effect to results. That means it is a stable method to be used in REST.

However, TSVD is a filter, while filters out the high frequency noise, some useful information is also lost. In essence, we sacrifice some information for a better smoothness of the solution. Other methods have been developed not by completely removing the singular values, but by modifying them so that they can contribute to the information content. Such methods [15] could be adopted in further investigations to restrain the reconstruction error.

Furthermore, REST needs more practical tests in EEG practice to prove out its effectiveness and feasibility.

Acknowledgments

This work is supported by the NSFC (No. 90208003), the National 973 Research Project No. 2003CB716106, the Key Project of Science and Technology of MOE PRC (No. 02065), Doctor training Fund of MOE, PRC and TRAPOYT.

References

[1] J.E. Desmedt, V. Chalklin, C. Tomberg, Emulation of somatosensory evoked potential (SEP) components with the 3-shell head model and the problem of 'ghost potential fields' when using an average reference in brain mapping, Electroenceph. Clin. Neurophysiol. 77 (1990) 243—258.

[2] E. Niedermeyer, F. Lopes Da Silva, Electroencephalography Basic Principles, Clinical Applications and Related Fields, fourth edition, Williams and Wilkins, Baltimore, MD, 1999.

[3] D.B. Geselowitz, The zero of potential, IEEE Eng. Med. Biol. 1 (1998) 128—132.

[4] J.R. Wolpaw, C.C. Wood, Scalp distribution of human auditory evoked potentials. I. Evaluation of reference electrode sites, Electroenceph. Clin. Neurophysiol. 54 (1982) 15—24.

[5] R.D. Pascual-Marqui, D. Lehmann, Topographical maps, sources localization inference, and the reference electrode, Clin. Neurophysiol. 88 (1993) 532—533, comments on a paper by Desmedt et al.

[6] D. Yao, A method to standardize a reference of scalp EEG recordings to a point at infinite, Physiol. Meas. 22 (2001) 693—711.

[7] D. Yao, The equivalent source technique and cortical imaging, Electroenceph. Clin. Neurophysiol. 98 (1996) 478—483.

[8] D. Yao, High-resolution EEG mappings: a spherical harmonic spectra theory and simulation results, Clin. Neurophysiol. 111 (2000) 81—92.

[9] R. Srebro, R.M. Oguz, K. Hughlett, P.D. Purdy, Estimating regional brain activity from evoked potential field on the scalp, IEEE Trans. Biomed. Eng. 40 (1993) 509—516.

[10] Y.C. Cai, D. Yao, A method to calculate source potential in realistic head model and its effectiveness, J. UESTC China 32 (2003) 149—154.

[11] R. Sidman, D. Vincent, D. Smith, L. Lee, Experimental tests of the cortical imaging technique applications to the response to median nerve stimulation and the localization of epileptiform discharges, IEEE Trans. Biomed. Eng. 39 (1992) 437—444.

[12] H. Johan, Improving the accuracy of the boundary element method by the use of second-order interpolation functions, IEEE Trans. Biomed. Eng. 47 (2000) 1336—1346.

[13] T.F. Oostendorp, J. Delbeke, D.F. Stegeman, The conductivity of the human skull: results of in vivo and in vitro measurements, IEEE Trans. Biomed. Eng. 47 (2000) 1487—1492.

[14] D. Yao, High-resolution EEG mapping: an equivalent charge layer approach, Phy. Med. Biol. 48 (2003) 1997—2011.

[15] A. Kirsch, An introduction to the mathematical theory of inverse problems, Springer-Verlag, New York, 1996.